BNL-101578-2014-TECH

RHIC/PG/35;BNL-101578-2013-IR

Need For Heidelberg Linac

G. R. Young

January 1984

Collider Accelerator Department

Brookhaven National Laboratory

U.S. Department of Energy

USDOE Office of Science (SC)

DISCLAIMER

RHIC-PG-35

NEED FOR HEIDELBERG LINAC

Glenn Young
March 2, 1984

(BNL, January 16, 1984)

3/1/84

Need for Heidelberg LINAC

The point of this note is to look once more at the net current out of the booster as a function of injection energy.

Now that stripping efficiency numbers are available for gold from H Wegner's recent Bevalac run, a check can be made of expected currents out using known efficiencies for all three required strippers.

The argument is as follows. The booster has a given maximum $B\rho$. The charge state of the gold injected is a strong function of injection energy. The ejection energy is a strong function of charge state and the stripping efficiency of gold to Au^{79+} is a strong function of booster output energy in the range we have been discussing. However, for a fixed number of turns injected and constant input current, the total number of particles in the booster is also a strong (decreasing) function of injection energy.

This note attempts to assemble all of this.

The "bottom line", is that for 2 stage tandem operation and 200 μA source output, 1.05 MeV/A is optimum injection energy and no LINAC is needed. For 400 μA source output, 1.7 MeV/A is optimum injection energy and the LINAC is needed.

Particles/bunch Out of Booster as a function of Injection Energy into Booster.

2/27/84

^{197}Au, Energy In vs Energy Out, For Booster

$2\pi R = 201.84\,m$; $\boxed{B\rho = 16.501\ T\text{-}m}$ $(1.2T\ @\rho = 13.751\ m)$

MeV/A in	β_{in}	Q_{MP} FOIL	β_{OUT}/β_{in}	MeV/A out	β_{OUT}	$\mathcal{E}_{STRIP}$ copper	N_8^{out} ($\times 10^9$)	N_{24}^{out} ($\times 10^9$)
0.563	.03475	30	18.09	266.5	.6288	32%	1.50	4.50
0.675	.03805	32	17.17	298.7	.6532	44%	1.89	5.66
0.802	.04147	34	16.29	332.1	.6757	54%	2.12	6.37
0.964	.04546	36	15.32	366.5	.6964	61%	2.19	6.56
1.178	.05024	38	14.24	402.0	.7156	69%	2.24	6.72
1.376	.05429	40	13.51	438.4	.7332	73%	2.19	6.58
1.624	.05897	42	12.71	475.6	.7495	79%	2.18	6.55
1.904	.06384	44	11.98	513.6	.7645	83%	2.12	6.36
2.234	.06913	46	11.26	552.4	.7784	86%	2.03	6.09
2.599	.07455	48	10.61	591.8	.7912	89%	1.95	5.84
3.046	.08067	50	9.96	631.9	.8031	91%	1.84	5.52
3.589	.08753	52	9.30	672.5	.8141	92%	1.71	5.14
4.188	.09451	54	8.72	713.6	.8242	93%	1.60	4.81
4.975	.10294	56	8.10	755.3	.8337	94%	1.49	4.47

$\mathcal{E}_{strip}$ included!

$\frac{\beta_{OUT}}{\beta_{in}}$ gives the range of RF frequency swing

$$N_8 = 8 \cdot \frac{201.84\ m}{\beta_{in} \cdot c} \cdot \frac{4.85\ p\mu A\ (Au)}{1.602\ 10^{-19}\ \text{part/coulomb}} \cdot \underline{\underline{\mathcal{E}_{STRIP}}}\ \text{particles}$$

$$N_{24} = 3 \cdot N_8$$

OK, but this is not a fair comparison yet, as there is a space charge limit for the lower injection energies which cuts down their final number of particles.

2/27/84

Now include the space charge limit

		$(\times 10^9)$				
MeV/A in	ϕ_{mp}^{Foil}	N_{sc}	$N_{sc} \cdot \varepsilon_{strip}$	N_8^{out}	N_{24}^{out}	#Turns
0.563	30	1.81	0.58	1.50	4.50	3.1
0.675	32	1.90	0.84	1.89	5.66	3.6
0.802	34	2.00	1.08	2.12	6.37	4.1
0.964	36	2.15	1.31	2.19	6.56	4.8
1.178	38	2.36	1.63	2.24	6.72	5.8
1.376	40	2.49	1.82	2.19	6.58	6.6
1.624	42	2.66	2.10	2.18	6.55	7.7
1.904	44	2.85	2.36	2.12	6.36	8.9
2.234	46	3.06	2.63	2.03	6.09	10.4
2.599	48	3.27	2.91	1.95	5.84	11.9
3.046	50	3.53	3.22	1.84	5.52	14.0
3.589	52	3.85	3.54	1.71	5.14	16.6
4.188	54	4.17	3.88	1.60	4.81	19.4
4.975	56	4.61	4.34	1.49	4.47	23.3
				from last page		to reach N_{sc}

$$\#\text{Turns} = \frac{N_{sc} \cdot \varepsilon_{strip}}{N_8^{out}} \cdot 8$$

i.e the number of turns to inject to reach the space charge limit at injection

So, if we are sure at least 8 turns can be injected, then the injection energy is the limit (via space charge) up to ≈ 1.8 MeV/A. At that point, cleverness in exceeding 8 turns into the booster is required.

2/28/84

However, one last factor must be included. The tandem can only produce ^{197}Au at 1MeV/A. To exceed this, we must include a 50% capture efficiency if we propose to use a MPI-type LINAC to boost the energy. The number for N_{sc} does not change, as it depends only on the entrance charge state, booster parameters and the injection energy. How you get the particles is your problem. But, N_8^{out} must be decreased by 50% above 1MeV/A if the linac is used, as proposed.

MeV/A in	Q_{mp}^{Foil}	$N_{sc} \cdot \varepsilon_{strip}$	N_8^{out} *	N_{24}^{out} *	# Turns
0.563	30	0.58	1.50	4.50	3.1
0.675	32	0.84	1.89	5.66	3.6
0.802	34	1.08	2.12	6.37	4.1
0.964	36	1.31	2.19	6.56	4.8
1.178	38	1.63	1.12	3.36	11.6
1.376	40	1.82	1.09	3.29	13.4
1.624	42	2.10	1.09	3.28	15.4
1.904	44	2.36	1.06	3.18	17.8
2.234	46	2.63	1.02	3.05	20.6
2.599	48	2.91	0.98	2.92	23.8
3.046	50	3.22	0.92	2.76	28.0
3.589	52	3.54	0.86	2.57	32.9
4.188	54	3.88	0.80	2.41	38.8
4.975	56	4.34	0.75	2.24	46.3

to reach $N_{sc} \cdot \varepsilon_{strip}$

2/28/84

Thus, the line to follow on the "TANDEM + LINAC" graph, to get the maximum particles/bunch out of the booster and into the AGS, is the "$N_{SC} \cdot \varepsilon_{STRIP}$" line up to 1.1 MeV/A and then the "8 TURN INJECTION" line after that. Thus for 2 stage tandem operation, injecting 5 turns to reach the space charge limit at 1.1 MeV/A gives the greatest booster output.

For ~~two~~ three-stage tandem operation, the optimum energy (see the "TANDEM ONLY" graph) is 1.7 MeV/A and requires 8 turn injection into the booster. However, three stage operation only produces (MP6 at −9 MV, MP7 at +15 MV) $^{197}Au^{17+}$ at 1.42 MeV/A. The space charge limit then corresponds to 7 turn injection.

So, it does not appear the MPI linac will help increase the net output of gold from the booster into the AGS.

NOTE ADDED 3/1/84

Harvey Wegner feels the source could be pushed to 400 μA instantaneous current. The result of this, for 8 turn booster injection, is shown on the "Dependence on source current" graph. Then, the turn over is at 1.7 MeV/A, which needs the Heidelberg LINAC. The result is ~ 2.1 x10⁹ gold ions/bunch. It needs to be checked if IBS causes problems with such a number of particles/bunch.

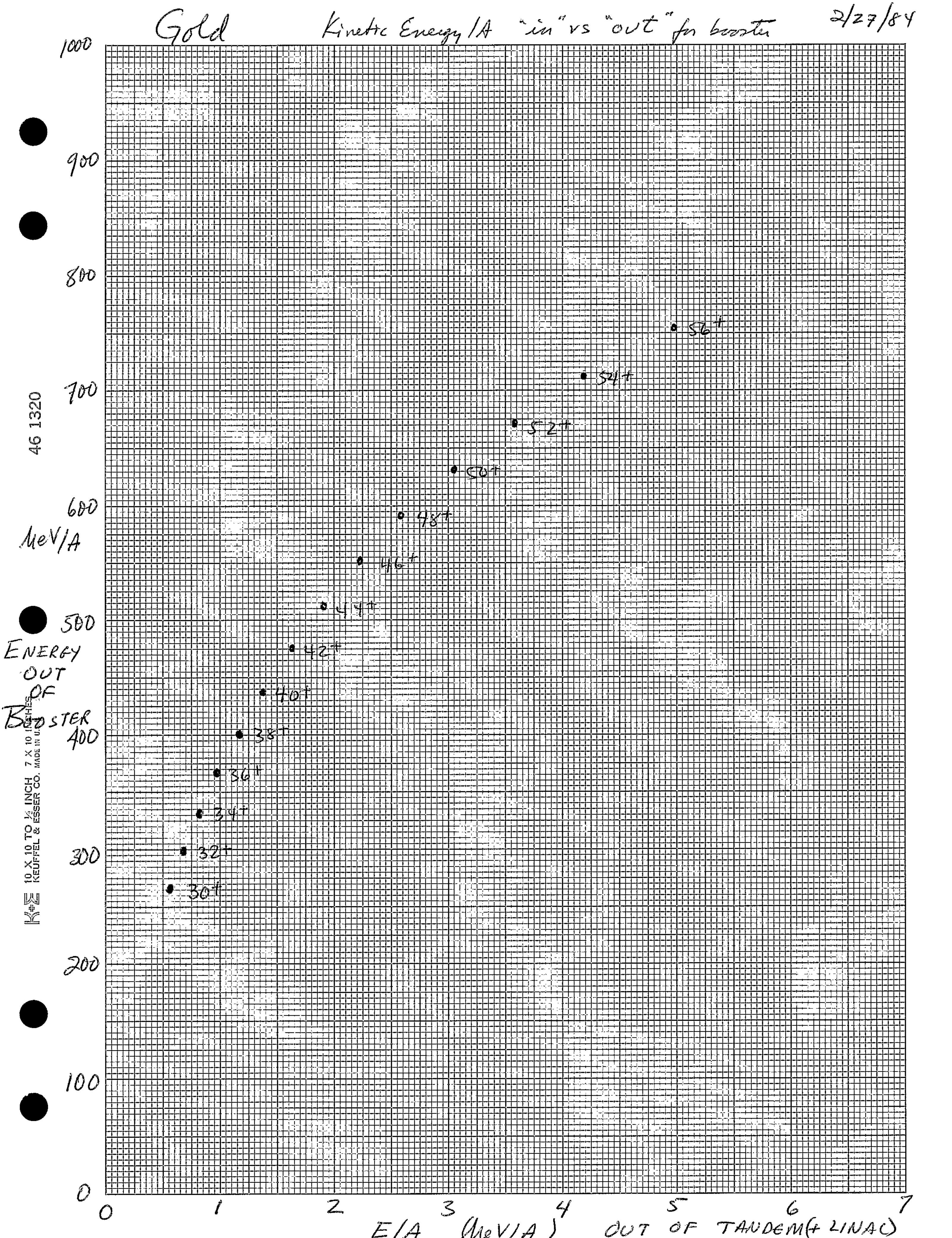
Gold
Kinetic Energy/A "in" vs "out" for booster
2/27/84
1000
900
800
700
600
MeV/A
500
ENERGY OUT OF BOOSTER
400
300
200
100
0
30+
32+
34+
36+
38+
40+
42+
44+
46+
48+
50+
52+
54+
56+
0
1
2
3
4
5
6
7
E/A (MeV/A) OUT OF TANDEM(+ LINAC)
46 1320
10 X 10 TO ½ INCH 7 X 10 INCHES
KEUFFEL & ESSER CO. MADE IN U.S.A.

2/28/84

Gold Kinetic Energy "In" vs RF FREQUENCY SWING

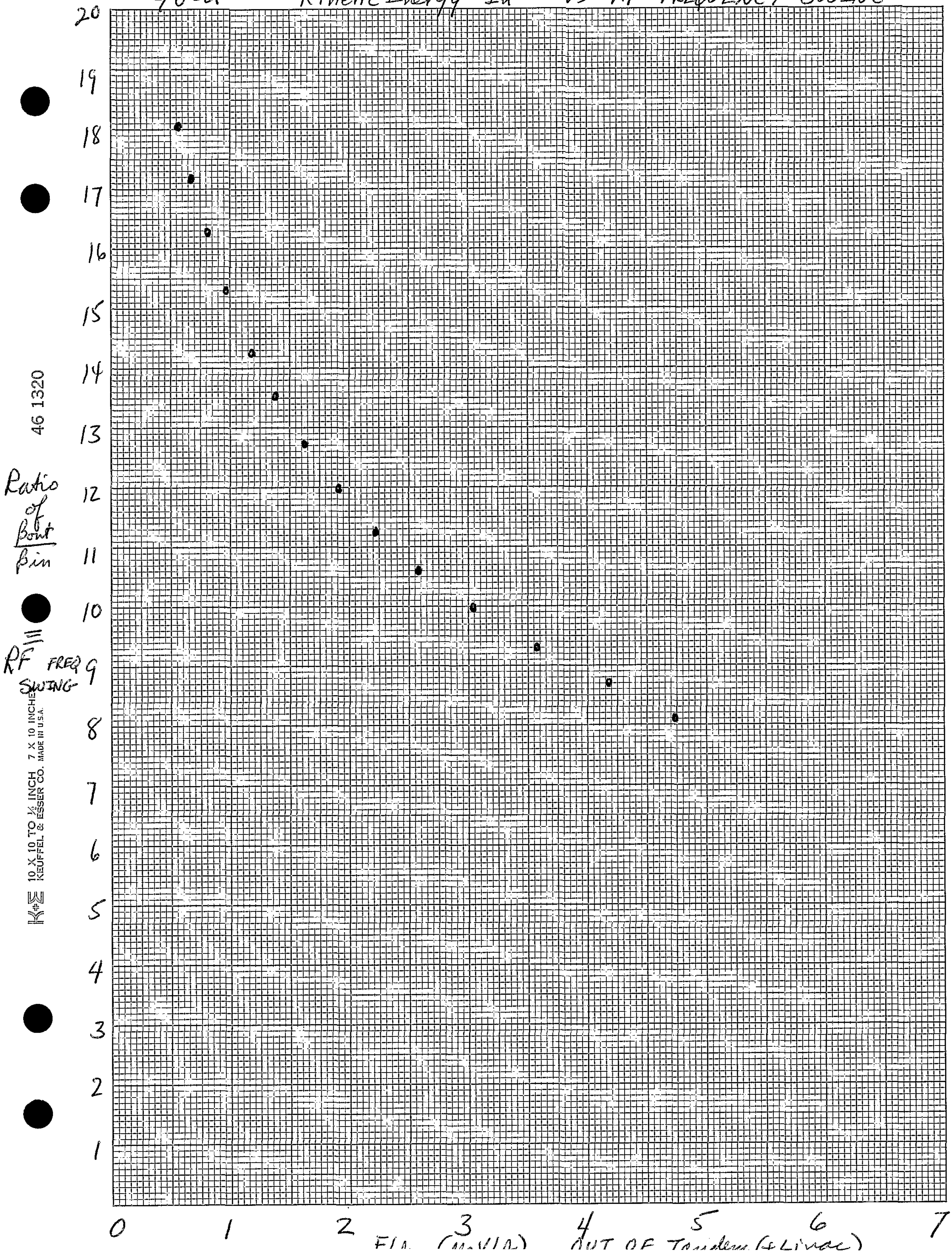

HGW 02/27/84

$^{197}Au^{61+}$ in

79+ out

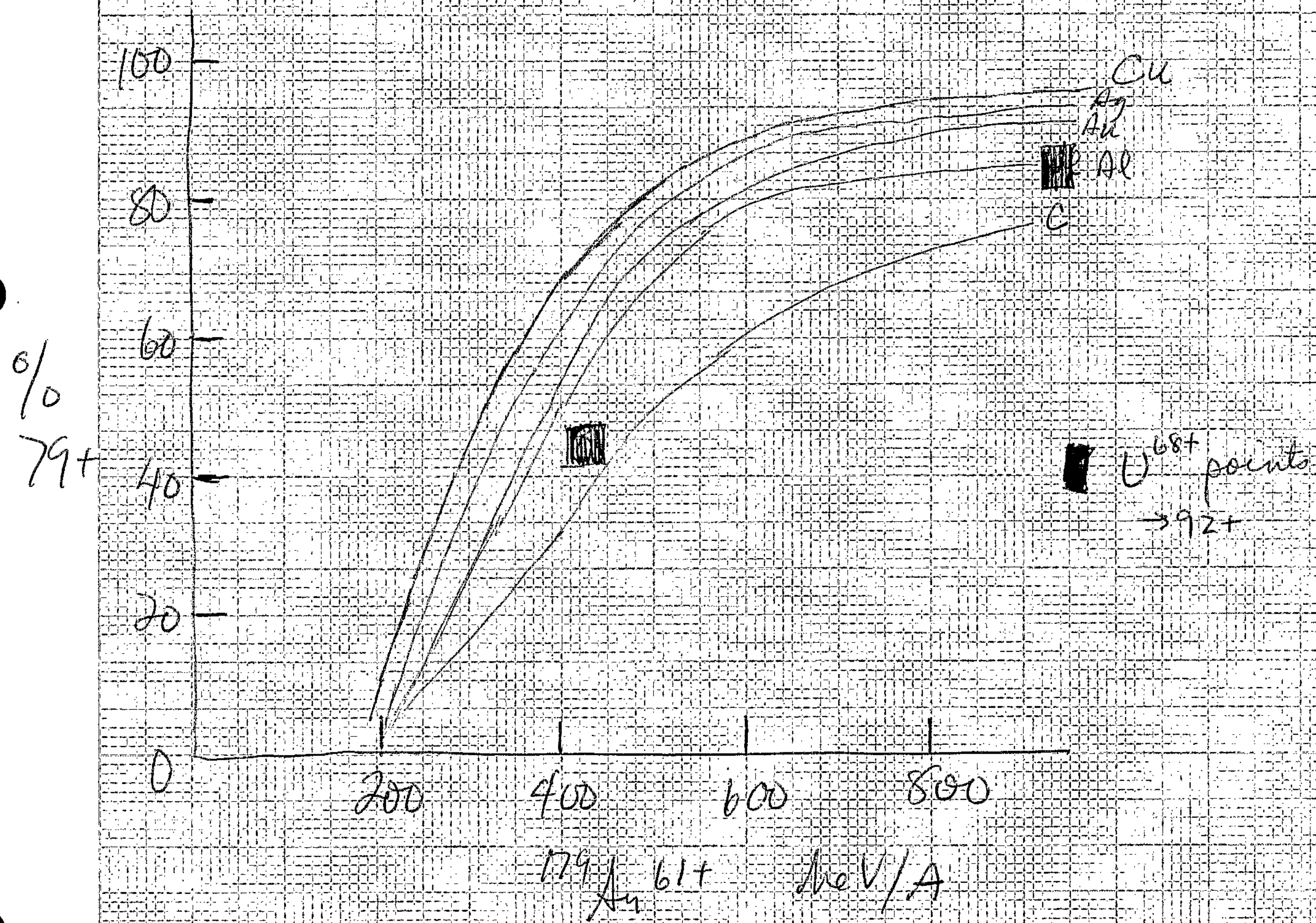

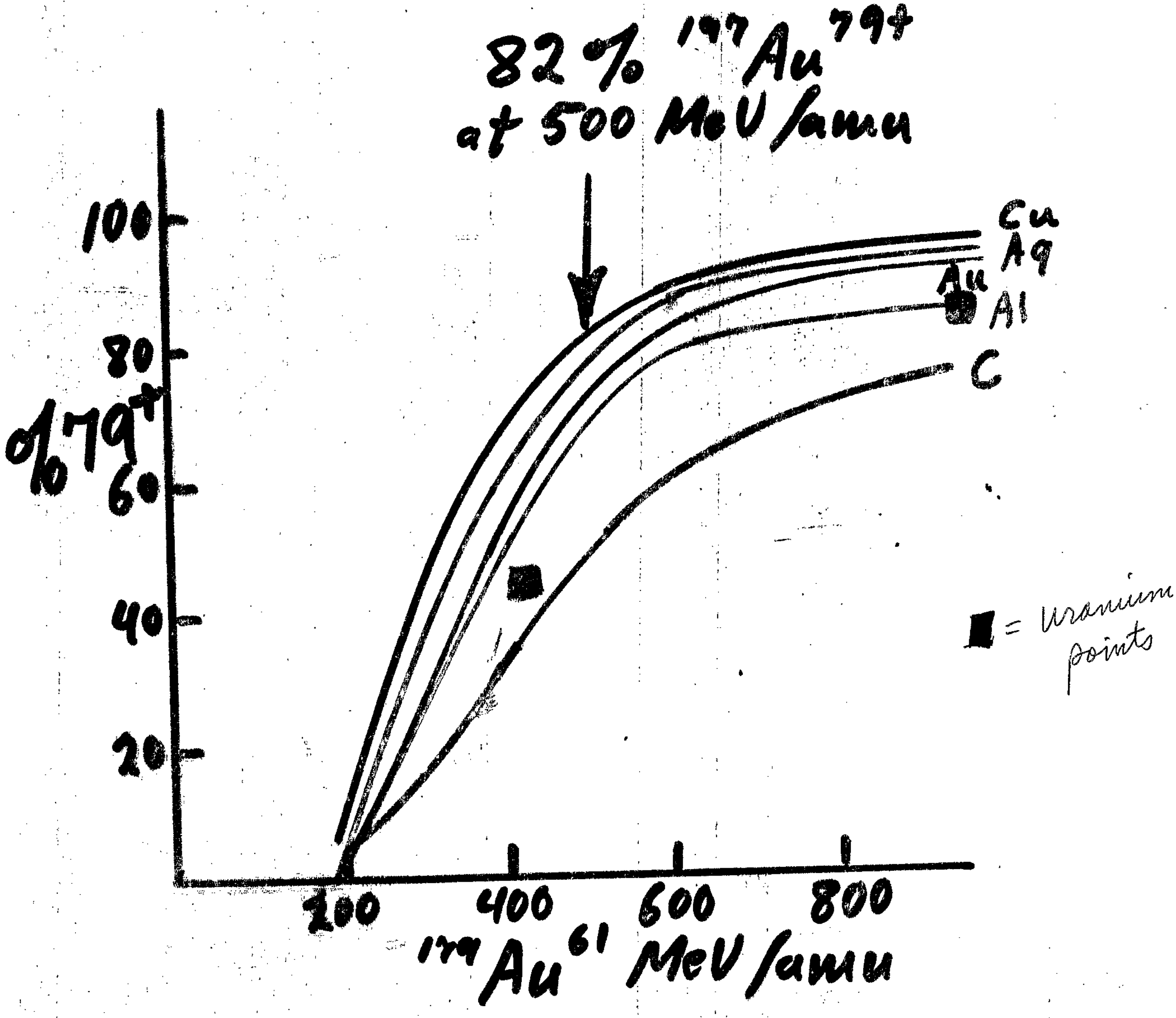

82% $^{197}Au^{79+}$
at 500 MeV/amu
100
80
60
40
20
% 79^{+}
Cu
Ag
Au
Al
C
■ = uranium points
200
400
600
800
$^{179}Au^{61}$ MeV/amu

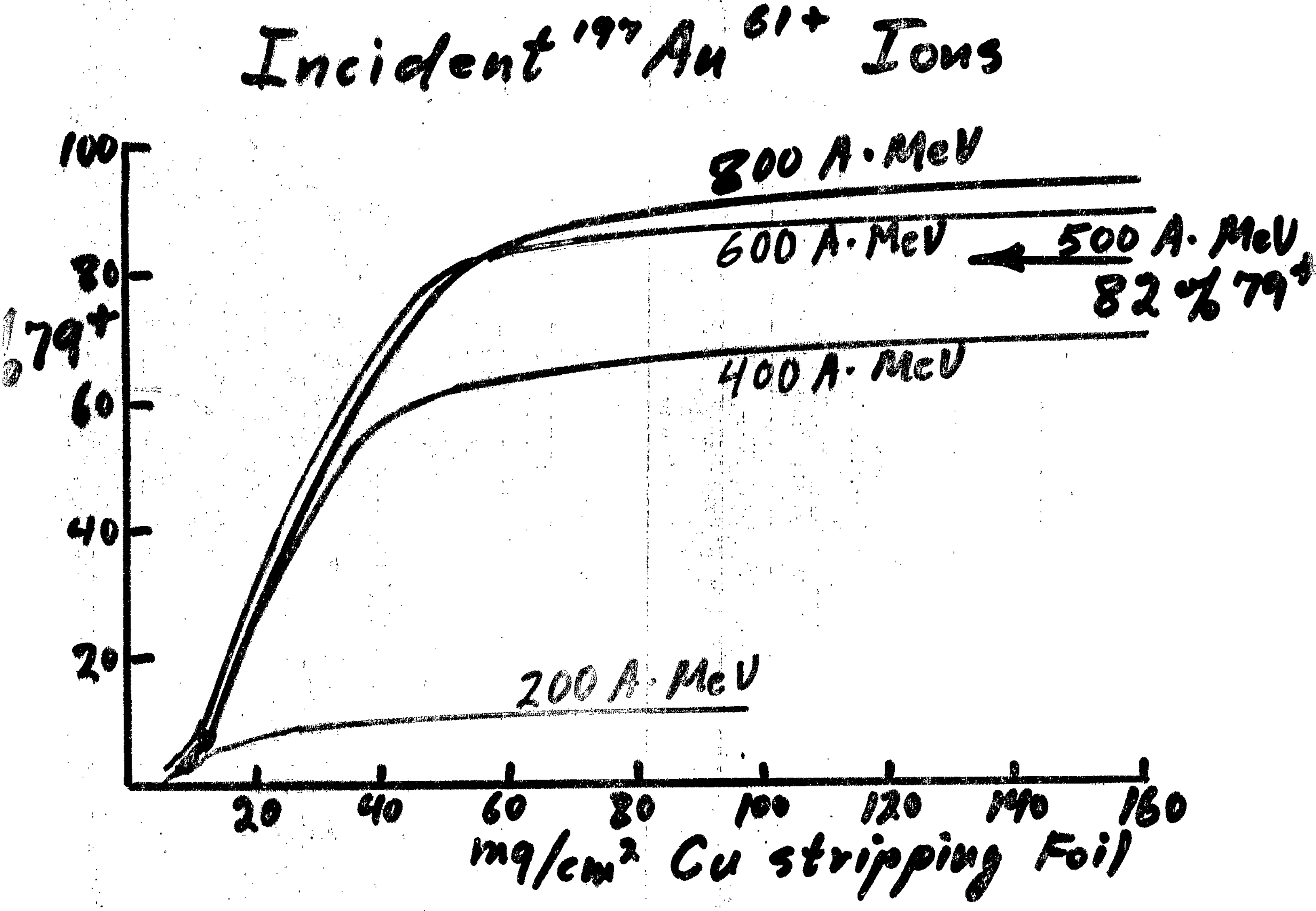

Incident $^{197}Au^{61+}$ Ions
800 A·MeV
600 A·MeV
500 A·MeV
82% 79+
400 A·MeV
200 A·MeV
% 79+
100
80
60
40
20
20
40
60
80
100
120
140
160
mg/cm² Cu stripping Foil

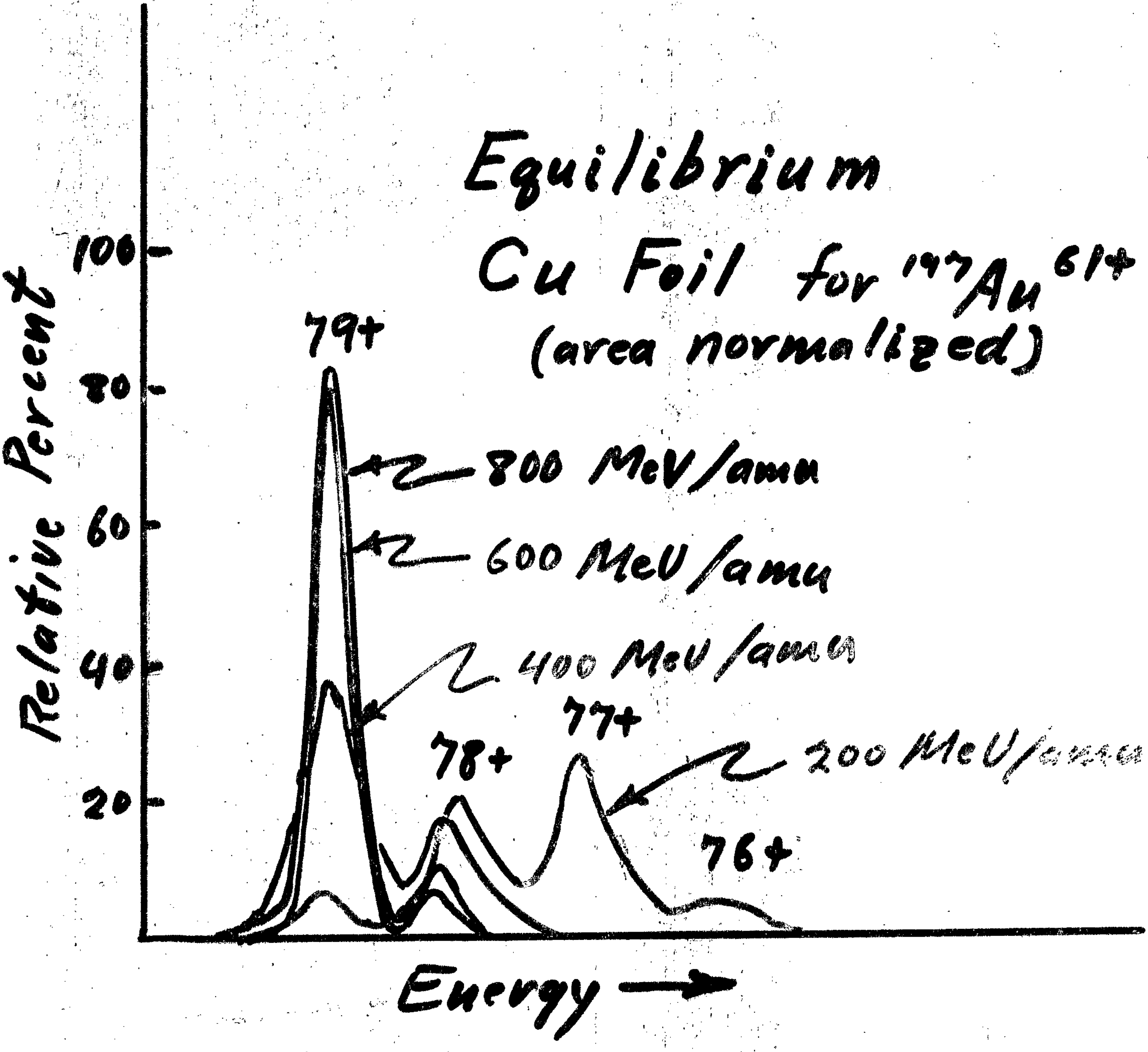

Equilibrium
Cu Foil for 197Au61+
(area normalized)
Relative Percent
100
80
60
40
20
79+
78+
77+
76+
800 MeV/amu
600 MeV/amu
400 MeV/amu
200 MeV/amu
Energy →

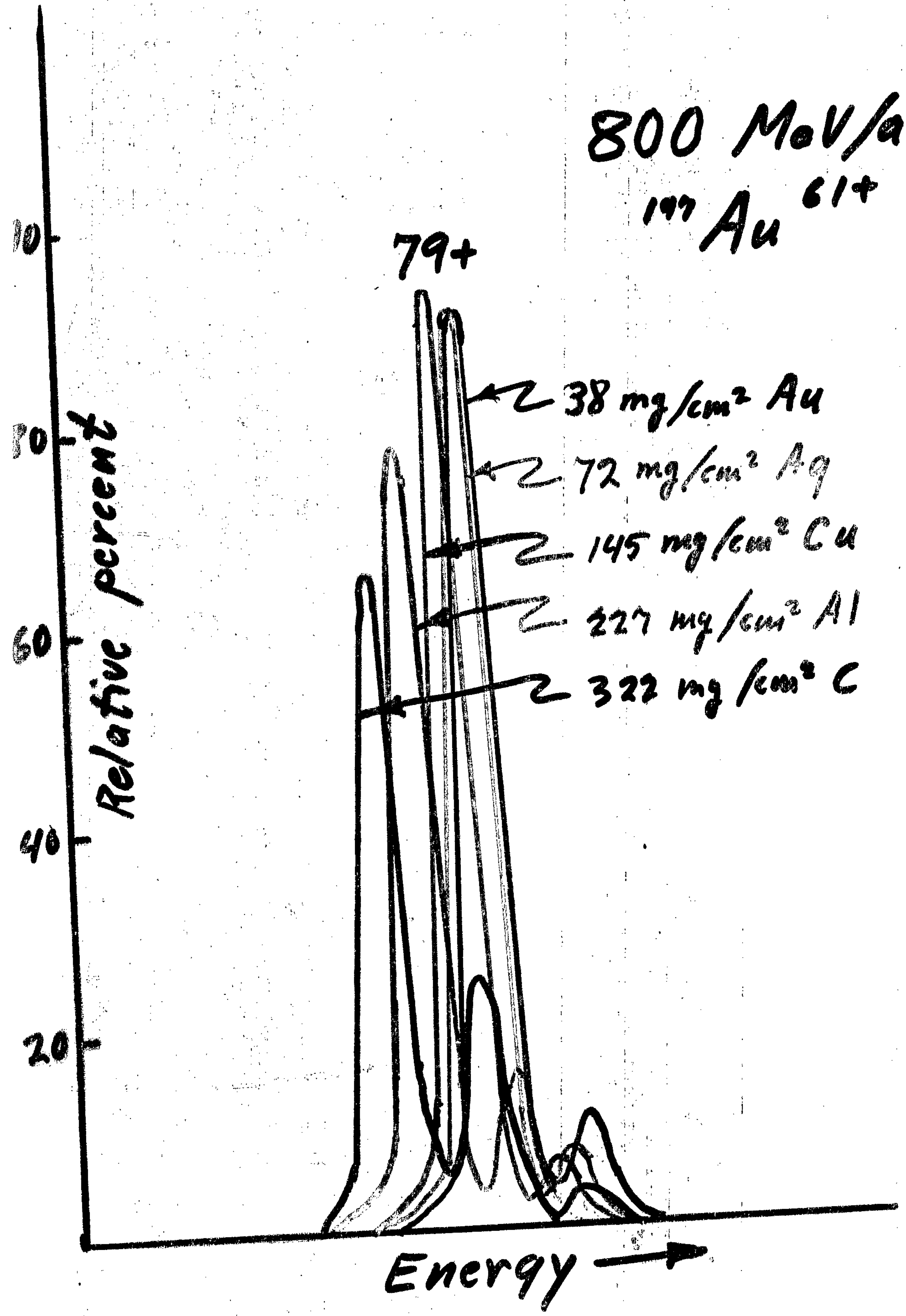

800 MeV/amu
197 Au 61+
79+
38 mg/cm² Au
72 mg/cm² Ag
145 mg/cm² Cu
227 mg/cm² Al
322 mg/cm² C
Relative percent
10
80
60
40
20
Energy

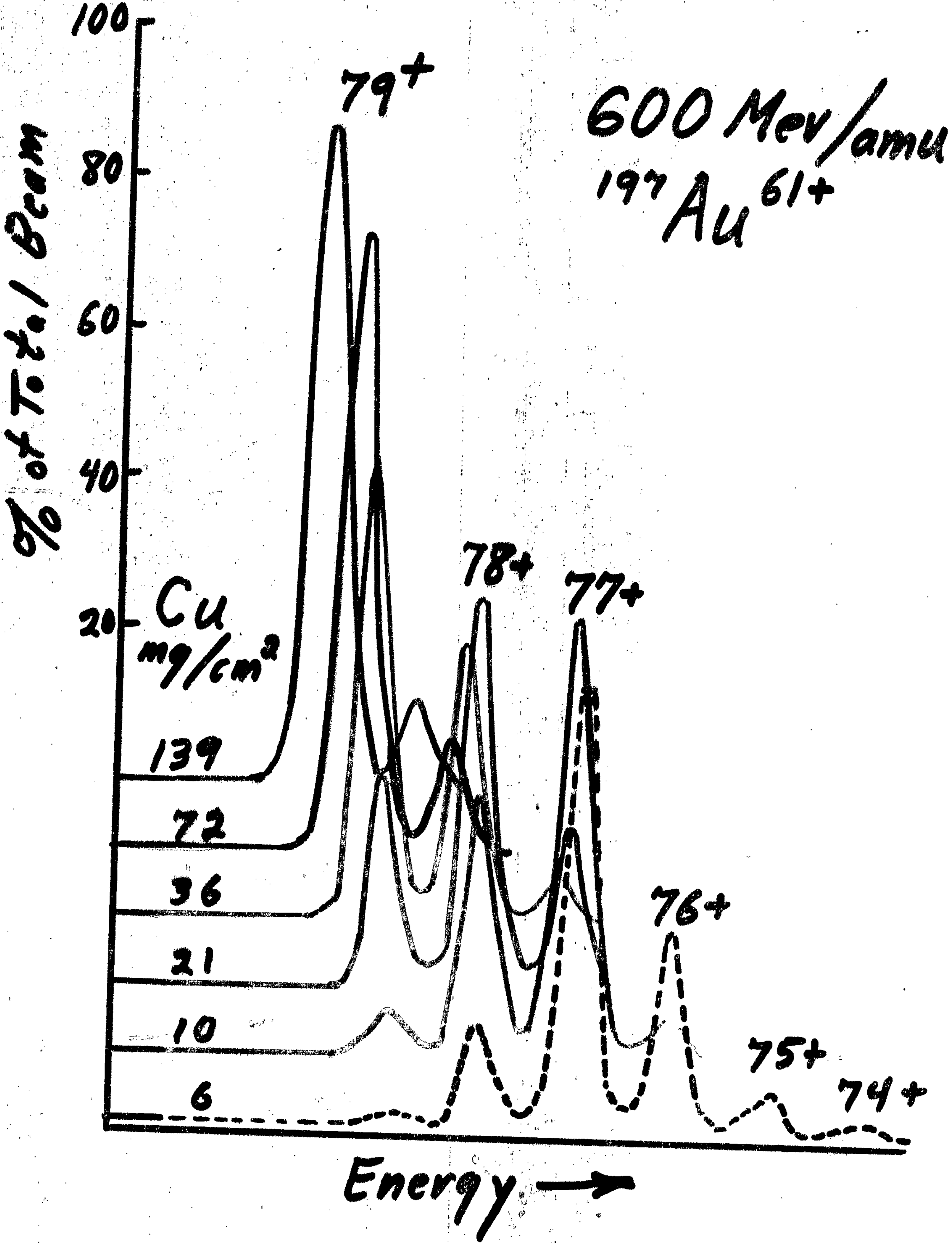

600 Mev/amu
$^{197}Au^{61+}$
% of Total Beam
100
80
60
40
20
Cu
mg/cm²
139
72
36
21
10
6
79+
78+
77+
76+
75+
74+
Energy →

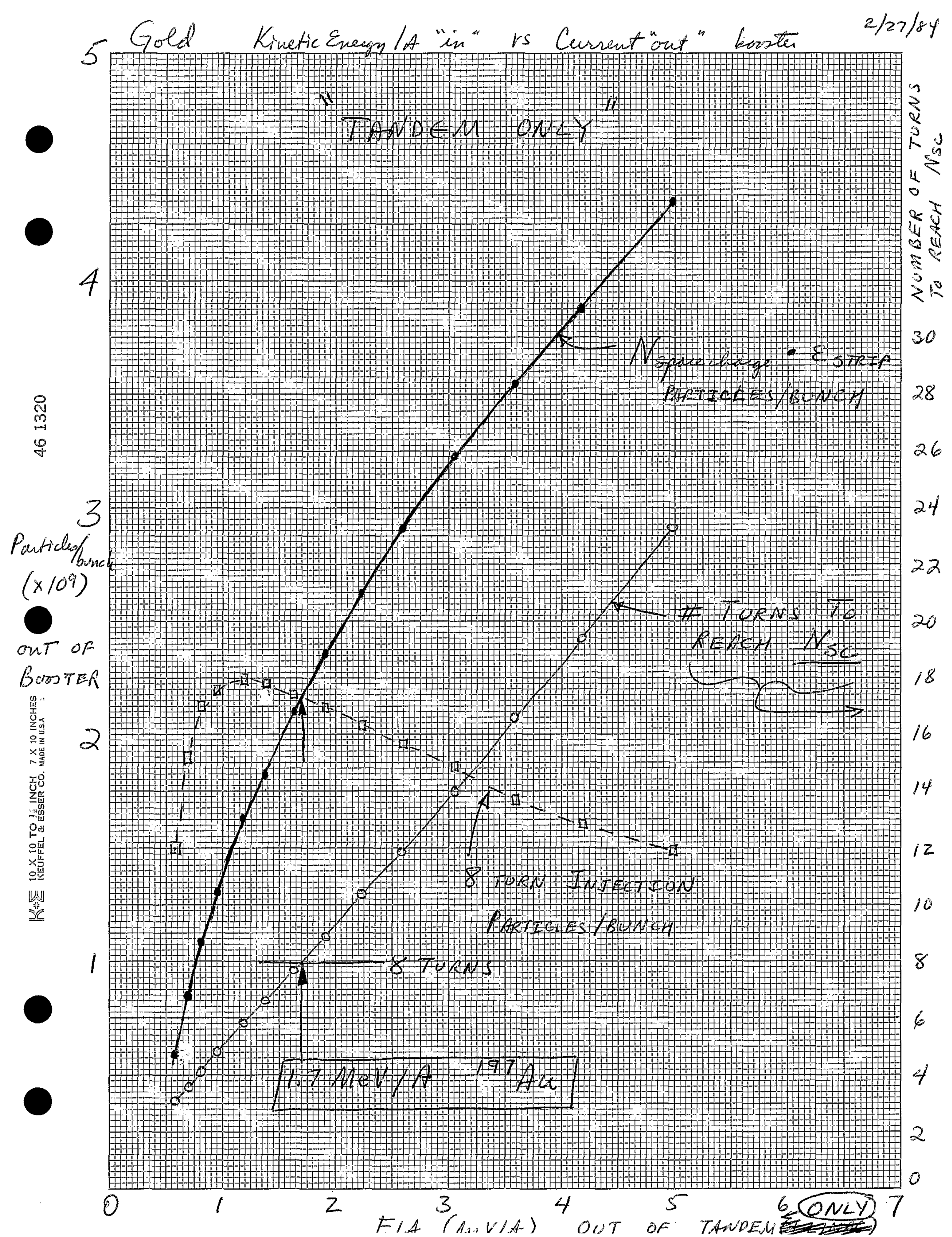
2/27/84
Gold Kinetic Energy/A "in" vs Current "out" booster
"TANDEM ONLY"
$N_{space\ charge} \cdot \varepsilon_{STRIP}$
PARTICLES/BUNCH
TURNS TO REACH N_{SC}
8 TURN INJECTION
PARTICLES/BUNCH
8 TURNS
1.7 MeV/A ^{197}Au
Particles/bunch
(x10⁹)
OUT OF BOOSTER
NUMBER OF TURNS TO REACH N_{SC}
E/A (MeV/A) OUT OF TANDEM (ONLY)
0
1
2
3
4
5
6
7
0
2
4
6
8
10
12
14
16
18
20
22
24
26
28
30
46 1320
K+E 10 X 10 TO 1/2 INCH 7 X 10 INCHES KEUFFEL & ESSER CO. MADE IN U.S.A.

Gold Kinetic Energy/A "In" vs Current "OUT" of Booster 2/28/84

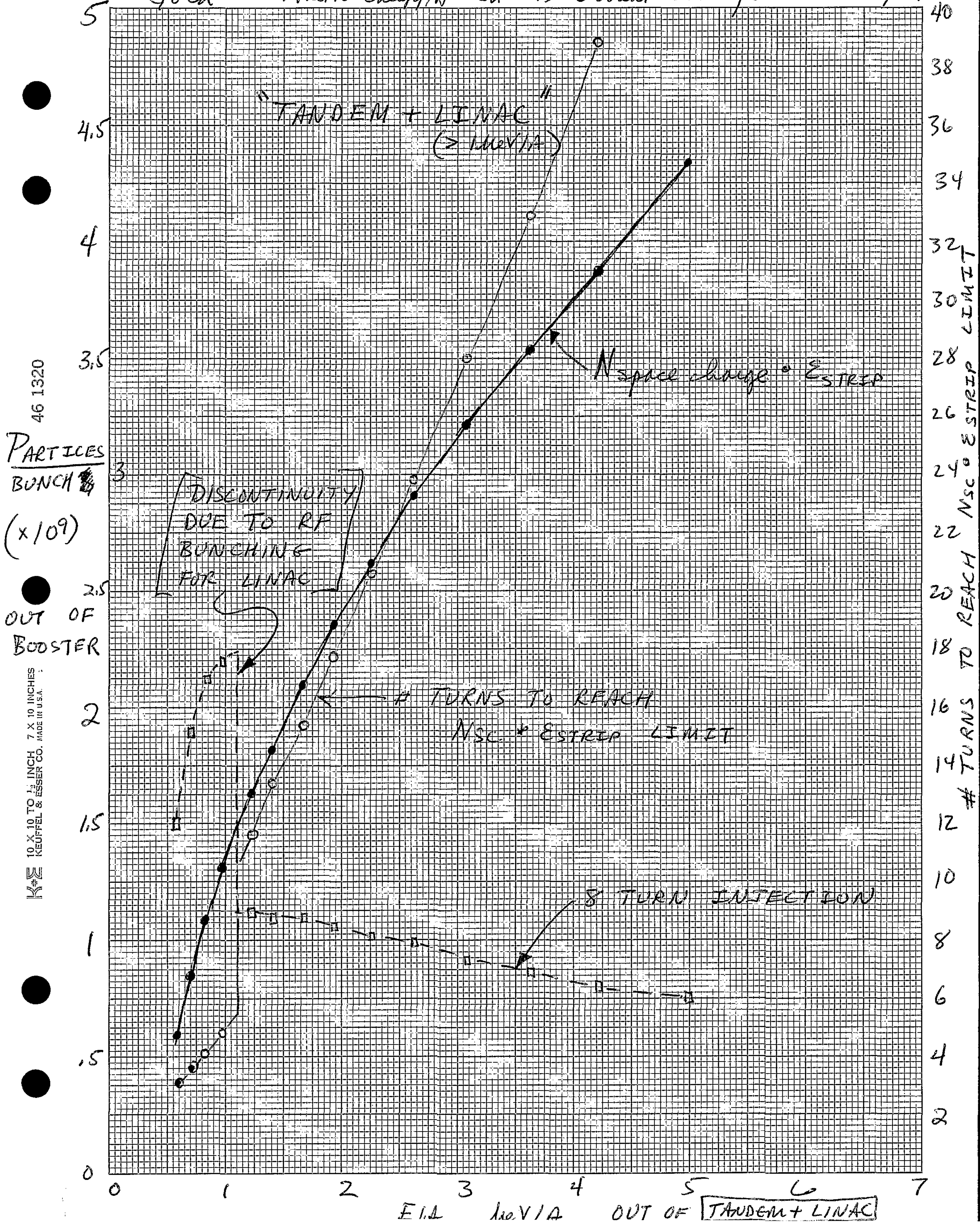

Gold Kinetic Energy "In" vs Current "Out" of Booster 3/1/84

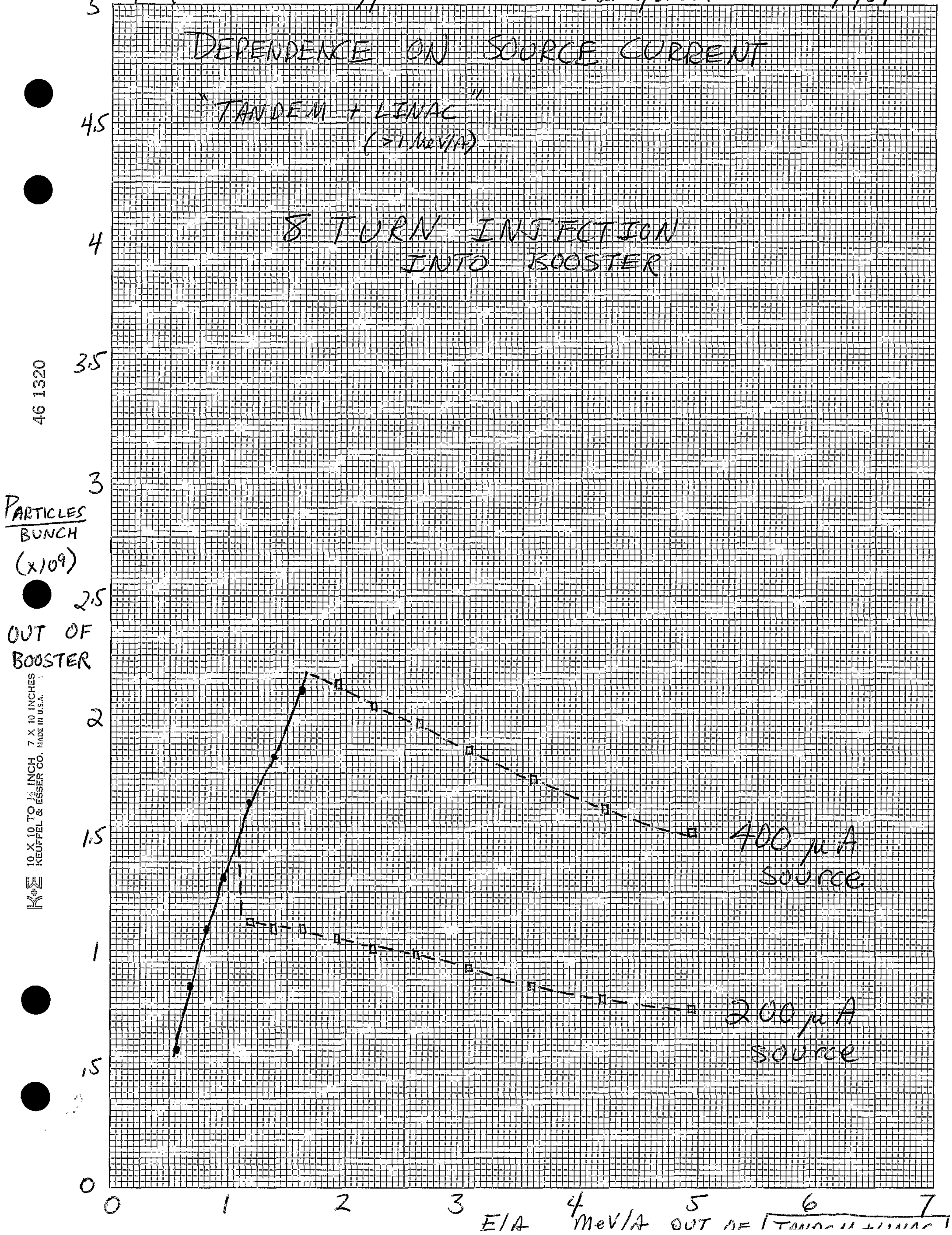

Electron Capture by U^{91+} and U^{92+} and Ionization of U^{90+} and U^{91+}

Harvey Gould
Materials and Molecular Research Division, Lawrence Berkeley Laboratory, University of California, Berkeley, California 94720
and
Douglas Greiner, Peter Lindstrom, and T. J. M. Symons
Nuclear Science Division, Lawrence Berkeley Laboratory, University of California, Berkeley, California 94720
and
Henry Crawford
Space Sciences Laboratory, University of California, Berkeley, California 94720
(Received 8 August 1983)

Experimental cross sections at energies of 962 and 437 MeV/nucleon are reported for $U^{92+} \rightleftarrows U^{91+}$ and $U^{91+} \rightleftarrows U^{90+}$ in Mylar, Cu, and Ta, as well as equilibrium charge-state distributions in these materials. At 962 MeV/nucleon a beam containing over 85% bare U^{92+} nuclei is obtained.

PACS numbers: 34.70.+e, 29.25.Cy, 34.50.Hc

A knowledge of the electron-capture and ionization cross sections for relativistic very heavy ions has application to the determination of nuclear charge from energy-loss measurements —where the rate of energy loss is charge-state dependent—and to the design of an ultrarelativistic heavy-ion accelerator—where the use of higher charge states allows for a smaller and more energy-efficient accelerator.

In this Letter we report measurements, at energies of 962 and 437 MeV/nucleon, of the cross sections for the capture of an electron by U^{92+} and U^{91+} and for the ionization of U^{91+} and U^{90+} in Mylar, Cu, and Ta. These are the first experimental cross sections for capture and loss of an electron by a relativistic heavy ion of nuclear charge >18. We find that beams containing nearly 50% bare U^{92+} are produced by stripping 437-MeV/nucleon uranium in a 90-mg/cm^2 Cu target and that beams containing over 85% bare U^{92+} are produced by stripping 962-MeV/nucleon uranium in 150-mg/cm^2 Cu or 85-mg/cm^2 Ta targets.

Relativistic U^{68+} ions are obtained from the Lawrence Berkeley Laboratory Bevalac[1]—a heavy-ion linear accelerator (Super-HILAC) and a synchrotron (Bevatron) operating in tandem. After extraction from the Bevalac, the U^{68+} ions pass through a Mylar ($C_5H_4O_2$), Cu, or Ta target located upstream of a magnetic spectrometer. The resulting uranium charge states are spatially separated in the magnetic spectrometer and detected by a position-sensitive proportional counter. At the proportional counter, the separation between adjacent uranium charge states is about 1 cm. The convolution of the beamwidth and the position resolution of the proportional counter is about 0.2 cm full width at half maximum. An energy loss of a few percent or less is observed for uranium ions in targets of sufficient thickness to produce a near-equilibrium charge-state distribution. No increase in the beam width is observed.

We determine the cross sections for capture and ionization by a least-squares fit[2] of single-electron capture and loss cross sections to curves of the relative charge-state populations of U^{89+}–U^{92+} versus target thickness (Fig. 1). This is a model-independent fit which is blind

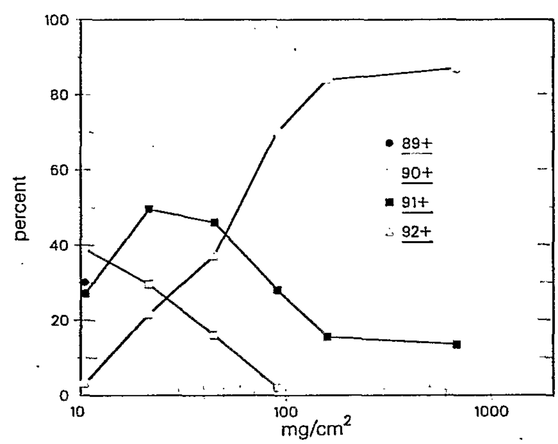

FIG. 1. Observed charge-state distributions of 962-MeV/nucleon uranium (incident charge state 68+), after passing through copper targets, as a function of target thickness.

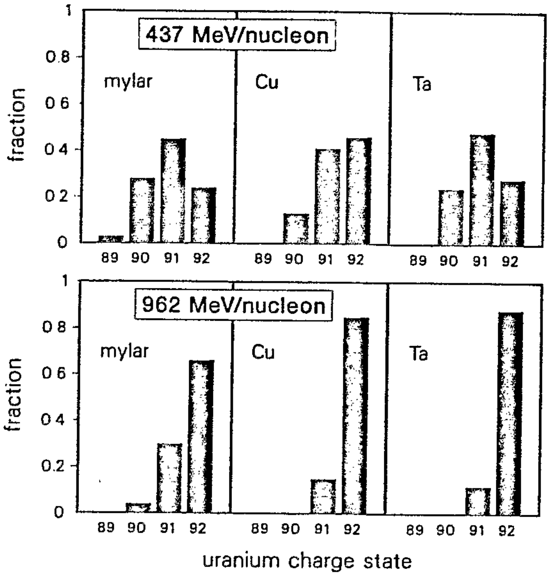

FIG. 2. Charge-state distributions of uranium at energies of 962 and 437 MeV/nucleon for equilibrium-thickness targets of Mylar ($Z_T \approx 6.6$), Cu ($Z_T = 29$), and Ta ($Z_T = 73$). At 437 MeV/nucleon, Cu produces higher charge states than does Ta.

to the atomic states involved and to the mechanisms for capture and loss.

The equilibrium charge-state distributions (Fig. 2) are determined from the ratios of capture and ionization cross sections. Using the cross-section ratios avoids extrapolation to infinite-thickness targets. For all energies and targets one or more targets were of near-equilibrium thickness. The difference between the charge-state distributions observed for our thickest Cu and Ta targets and the equilibrium distributions for these materials was less than 5% of the total counts. The use of extremely thick targets offers no advantage over our present method because of the slowing down of the uranium in the target. We estimate the uncertainty in determining the equilibrium distributions, mostly due to statistics and a small background, to be less than 5% of the total counts.

The *absolute* cross sections, shown in Figs. 3 and 4, have an estimated error of a factor of 2.

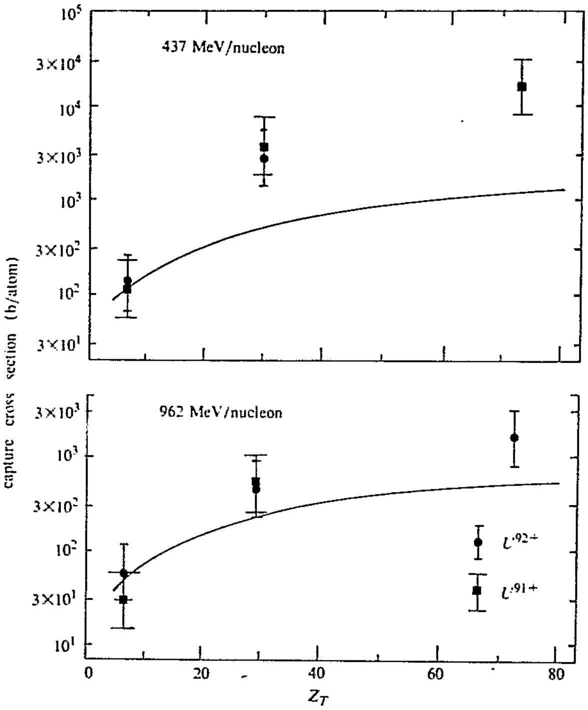

FIG. 3. Cross sections for capture of an electron by U^{92+} and U^{91+} at energies of 962 and 437 MeV/nucleon as a function of Z_T. Experimental points are for Mylar ($Z_T \approx 6.6$), Cu ($Z_T = 29$), and Ta ($Z_T = 73$). σ_{REC} for U^{92+}, calculated from Eq. (1), is shown as the continuous curve.

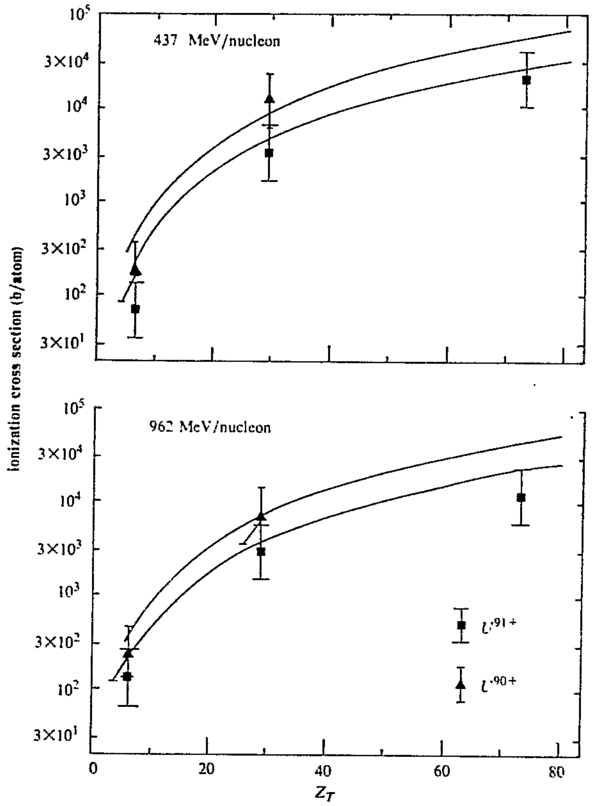

FIG. 4. Cross sections for ionization of U^{91+} and U^{90+} at energies of 962 and 437 MeV/nucleon as a function of Z_T. Experimental points are for Mylar ($Z_T \approx 6.6$), Cu ($Z_T = 29$), and Ta ($Z_T = 73$). The continuous curves are the loss cross sections calculated from Eq. (2) for U^{91+} (upper curve) and U^{90+} (lower curve).

The error is relatively large because only a few targets were used to cover a large range of target thicknesses and the useful data for determining the cross sections are limited to from three to six (average 4.2) charge-state distributions.

Figure 3 shows the experimental cross sections for capture of an electron by U^{92+} and U^{91+} at energies of 962 and 437 MeV/nucleon in Mylar (effective $Z_T \approx 6.9$), Cu ($Z_T = 29$), and Ta ($Z_T = 73$). Relativistic uranium captures electrons by radiative electron capture (the inverse of photoionization) and by charge exchange. We first consider radiative electron capture. With neglect of binding energy of the target-atom electrons, the cross section[3] per target electron for radiative electron capture, σ_{REC}/electron, may be written in terms of σ_φ, the photoionization cross section, and X, the fraction of the shell of the uranium atom which is unoccupied:

$$\frac{\sigma_{REC}}{\text{electron}} = \frac{[(\gamma-1)+B_n/mc^2]^2 X \sigma_\varphi}{[\gamma+2B_n/mc^2]^2-1}. \tag{1}$$

Here B_n is the binding energy of an electron in the nth shell, m is the electron mass, and c is the speed of light. Also, $\gamma = (1-\beta^2)^{-1/2}$ and $\beta = v/c$, where v is the uranium velocity. At 962 MeV/nucleon ($\gamma \approx 2.0$) and at 437 MeV/nucleon ($\gamma \approx 1.5$) photon energies from radiative electron capture into the K shell are 0.66 and 0.37 MeV, respectively. (Capture into higher shells lowers the photon energies by ≈ 0.1 MeV.) The total cross sections for photoionization[4] of all shells by 0.66- and 0.37-MeV photons are 25 and 90 b, respectively. Multiplying by the number of electrons in the target atom, we obtain values of σ_{REC} for U^{92+} shown in Fig. 3. σ_{REC} for U^{91+} is about half as large.

The second process for electron capture is nonradiative charge exchange. Precise calculations of the relativistic cross sections for nonradiative charge exchange with a complex target atom are not yet available. Present calculations[5] of the charge-exchange cross sections from hydrogenlike targets by 962- and 437-MeV/nucleon U^{92+} find a strong dependence on the nuclear charge of the target. In low-Z_T targets these cross sections are much smaller than σ_{REC} and in high-Z_T targets they are somewhat larger.

With the assumption of a negligible contribution to the capture cross section from nonradiative charge exchange in Mylar, our experimental data for Mylar are in satisfactory agreement with σ_{REC} calculated from Eq. (1). The difference between the experimental capture cross section and σ_{REC} for heavier targets in Fig. 3 is consistent with the increasing importance of nonradiative charge exchange for increasing Z_T and decreasing projectile energy.

To calculate the cross sections for ionization of U^{90+} and U^{91+}, we note that the relativistic Bethe theory[6,7] for energy loss by a heavy charged particle in matter predicts the cross sections for ionization and excitation of the target by the projectile. Reversing the role of the target and the projectile, we calculate the cross section (σ_i) for ionization of $U^{90+,91+}$:

$$\sigma_i = 4\pi a_0^2\left(\frac{\alpha}{\beta}\right)^2 \frac{1}{B_K}(Z_T^2+Z_T)f_K\left\{\ln\frac{(2\beta\gamma/\alpha)^2}{(0.048\,B_K)}\right\}. \tag{2}$$

Here a_0 is the Bohr radius of hydrogen, α is the fine-structure constant, B_K is the binding energy of a K-shell electron in units of rydbergs (1 Ry ≈ 13.6 eV). The quantities β and γ have the same meaning as in Eq. (1), Z_T is again the nuclear charge of the target, and f_K is a constant times the oscillator strength for transitions from the K shell to the continuum: $f_K = 0.29$ and 0.58 for U^{91+} and U^{90+}, respectively. Within the experimental error, the agreement in Fig. 4 between measured cross sections and cross sections calculated from the Bethe theory is satisfactory.

In conclusion, we find that beams containing more than 85% bare U^{92+} nuceli can be obtained by stripping U^{68+} in Cu and Ta targets of 150 mg/cm^2 and 85 mg/cm^2, respectively, and that beams containing about 50% bare U^{92+} nuclei can be obtained by stripping 437-MeV/nucleon uranium in 90 mg/cm^2 Cu. Our data are consistent with radiative electron capture being the dominant process at these energies for electron capture from light targets. It is clearly possible at these energies to produce beams of bare uranium nuclei for acceleration to ultrarelativistic energies and beams of few-electron uranium for atomic-physics tests of quantum electrodynamics.

We thank Mr. Douglas MacDonald, Mr. Ismael Flores, and Dr. Jose Alonso for their assistance in setting up the experiment and analyzing the data; and Professor Richard Marrus and Dr. Howel Pugh for their encouragement and support. We especially thank the operators and staff of the Bevalac whose skill and dedication made this experiment possible. This work was supported by the Director, Office of Energy Research; Office of Basic Energy Sciences, Chemical Sciences Division; and Office of High Energy and

Nuclear Physics, Nuclear Science Division, of the U. S. Department of Energy under Contract No. DE-AC-03-76SF00098, and by NASA.

---

[1]See, for example, J. R. Alonso *et al.*, Science 217, 1135 (1982).

[2]S. Datz, H. O. Lutz, L. B. Bridwell, C. D. Moak, H. D. Betz, and L. D. Ellsworth, Phys. Rev. A 2, 430 (1970).

[3]See for example, P. H. Fowler, V. M. Clapham, V. G. Cowen, J. M. Kidd, and R. T. Moses, Proc. Roy. Soc. London, Ser. A 318, 1 (1970).

[4]Cross sections were interpolated from values given by W. H. McMaster, N. Kerr Del Grande, J. H. Mallett, and J. H. Hubbell, *Compilation of X-Ray Cross Sections*, Lawrence Livermore Laboratory Report No. UCRL-50174, Sec. II. Rev. 1 (National Technical Information Service, U.S. Dept. Commerce, Springfield, Va., 1969), p. 344.

[5]R. Shakeshaft, Phys. Rev. A 20, 779 (1979); B. L. Moiseiwitsch and S. G. Stockman, J. Phys. B 13, 2975, 4031 (1980); D. H. Jakubassa-Amundsen and P. A. Amundsen, Z. Phys. A 298, 13 (1980).

[6]H. A. Bethe, Ann. Phys. (Leipzig) 5, 325 (1930); C. Møller, Ann. Phys. (Leipzig) 14, 531 (1932).

[7]Tests of the Bethe theory for ≈ 1-GeV/nucleon uranium and gold are reported by S. P. Ahlen and G. Tarlé, Phys. Rev. Lett. 50, 1110 (1983); and by C. J. Waddington, P. S. Freier, and D. J. Fixen, Phys. Rev. A 28, 464 (1983), respectively.